



Research article

Metformin exerts anti-liver fibrosis effect based on the regulation of gut microbiota homeostasis and multi-target synergy

Lianhua Kong^{a,1}, Juncong Ma^{b,1}, Li Dong^a, Chuanlong Zhu^a, Jie Zhang^{c,**}, Jun Li^{a,*}

^a Department of Infectious Disease, The First Affiliated Hospital of Nanjing Medical University, Nanjing, 210029, Jiangsu, China

^b Department of Emergency, Lian Shui People's Hospital, Huai'an, 223400, Jiangsu, China

^c Department of Endocrinology, The Affiliated Huai'an Hospital of Xuzhou Medical University, Huai'an, 223002, Jiangsu, China

ARTICLE INFO

Keywords:

Cell apoptosis
Inflammatory cytokines
Intestinal flora
Liver fibrosis
Metabolite
Metformin
Oxidative stress

ABSTRACT

Liver fibrosis can progress to cirrhosis if left untreated. Therefore, identifying effective anti-fibrotic drugs is crucial. This study aimed to investigate the role and potential mechanism of metformin in treating hepatic fibrosis based on the synergistic effect of multiple targets and the "intestine-liver axis" theory. A CCl₄-induced liver fibrosis mouse model was established. We measured liver function, liver fibrosis indicators, oxidative stress and inflammation indices. Hematoxylin and eosin and Masson's trichrome staining were used to detect collagen deposition. The expression of apoptotic proteins, TGF- β /Smads and TIMP-1/MMPs was assessed. 16S rRNA and untargeted metabolomics (liquid chromatography-mass spectrometry) were used to assess mouse intestinal flora and metabolites, performing a comprehensive correlation analysis. Metformin improved the general status and liver function and decreased liver collagen deposition in CCl₄-induced liver fibrotic mice. Compared with the control group, IL-6, TNF- α and COX-2 serum levels in the liver fibrosis group increased. Although not significantly different, the serum inflammatory marker levels in the metformin group were lower than those in the model group. Metformin decreased serum MDA and increased serum SOD activity, which increased and decreased, respectively, in the model group. Furthermore, metformin inhibited liver cell apoptosis, TGF- β 1 expression and TIMP-1, while promoting Smad7 expression, MMP-1 and MMP-2 in fibrotic mice. 16S rRNA analysis indicated that metformin significantly ameliorated the *Bacteroides*, *Helicobacter*, *Parabacteroides* and *Parasutterella* imbalance. We identified 385 differential metabolites between the metformin and model groups. *Prevotella* abundance significantly decreased in the metformin group and positively correlated with decreased taurocholic acid levels. Metformin potentially reverses liver fibrosis by inhibiting inflammation, mitigating oxidative stress damage and suppressing hepatocyte apoptosis via intestinal flora metabolite regulation. Metformin also regulates the TGF- β /Smads and TIMP-1/MMPs signalling pathways. This study provides a theoretical basis for the clinical use of metformin in patients with liver fibrosis.

* Corresponding author.

** Corresponding author.

E-mail addresses: zhangjie0771@163.com (J. Zhang), dr-lijun@vip.sina.com (J. Li).

¹ These authors contributed equally to this work.

1. Introduction

Liver fibrosis is caused by chronic liver injury, including chronic viral hepatitis, alcoholic liver disease, nonalcoholic fatty hepatitis and primary biliary cirrhosis. Extracellular matrix (ECM) deposition is a typical characteristic of liver fibrosis in various chronic liver diseases [1]. The accumulation of liver-injured myofibroblasts and an increase in ECM production are closely related to liver healing [2]. Early liver fibrosis is generally easy to reverse; however, if the underlying causative factors are left unattended over an extended period, liver fibrosis is likely to progress to cirrhosis [3]. Thus, the prompt removal or inhibition of stimulating factors, along with the implementation of appropriate interventions, are critical for reversing liver fibrosis. Currently, no agents are approved for reversing liver fibrosis. Thus, the identification of effective drugs that can prevent liver tissue damage and delay liver fibrosis is vital.

As a hypoglycaemic drug, metformin has been the focus of much research because of its role in regulating glycolipid metabolism in liver diseases. Extensive research has shown that metformin can improve hepatic function in nonalcoholic fatty liver disease and nonalcoholic steatohepatitis models. Metformin also has antifibrotic effects in various organs, independent of its lipid-lowering effects [4–6]. Although the anti-fibrotic effects of metformin have been well documented in both in vivo and in vitro preclinical experiments, clinical evidence for its efficacy in liver fibrosis remains lacking. Furthermore, the complex mechanisms by which metformin inhibits liver fibrosis in experimental studies remain unclear. Several factors contribute to the pathogenesis of liver fibrosis, including inflammation, oxidative stress, metabolic disorders and immunity [1]. In addition, metformin has been demonstrated to have anti-inflammatory, antioxidant and regulatory effects on metabolism and immunity, as well as other multi-target functions [7–9]. The role of gut microbiome-derived metabolites in the aetiology and iatrogenesis of liver fibrosis is becoming increasingly recognised with advances in omics technology. Cirrhosis and fibrosis are hypothesised to share a decrease in beneficial bacteria and an increase in potentially pathogenic bacteria [10,11]. In this study, it was investigated whether metformin has a therapeutic effect on mouse models of carbon tetrachloride 4 (CCL₄)-induced hepatic fibrosis, as well as its potential for clinical translation. Intestinal flora and metabolomics were then used to analyze the role of the “gut-liver axis” in metformin’s anti-liver fibrosis effects. This allowed us to comprehensively analyze the potential role of flora and metabolites in the progression of liver fibrosis. This research may provide a theoretical basis for the clinical application of metformin for liver fibrosis.

2. Materials and methods

2.1. Animal models

Thirty male C57BL/6J mice were purchased from Changzhou Cavens Laboratory Animal Co., LTD. and housed with laboratory chow and tap water at 22 ± 2 °C with 55 ± 5 % humidity and 12-h light-dark cycle and fed with standard chow diet and water. This study was reviewed and approved by the Experimental Animal Ethics Committee of Nanjing Medical University, with the approval number: IACUC-1201011. The mice were acclimated for one week before being randomly assigned to one of three groups, each with 10 mice, including a blank control group (control), a model group (model) and a metformin group (Dimethylbiguanide, DMBG). A mouse model of hepatic fibrosis was established by intraperitoneal injection of carbon tetrachloride (CCL₄, Maclin Shanghai, China). Olive oil (Maclin, Shanghai, China) was used to dissolve CCL₄ at a volume ratio of 1:3. Mice in the hepatic fibrosis model and DMBG treatment groups were intraperitoneally injected with 4 μ L/g body weight twice a week. The metformin group received 0.1% metformin in water and special attention was paid to modifying the daily water intake. Mice were euthanized after 6 weeks and relevant detection was performed (eight individuals were selected from each group).

2.2. The detection of serum biochemical indicators

A Rayto automatic biochemical analyzer was used to measure the levels of blood aspartate aminotransferase (AST) and glutamic-pyruvic transaminase (ALT) levels, following the instructions provided by the manufacturer. The four types of liver fibrosis were evaluated using procollagen III (PCIII), collagen type IV, (IV-C), laminin (LN) and hyaluronic acid (HA). Oxidative stress indicators. The concentrations of superoxide dismutase (SOD), malondialdehyde (MDA) and glutathione peroxidase (GSH) were. Interleukin-6 (IL-6), tumor necrosis factor- α (TNF- α) and cyclooxygenase-2 (COX-2) were detected according to the instructions of the ELISA kit (Nanjing Jiancheng Bioengineering Institute, Nanjing, CN).

2.3. Hematoxylin-eosin (H&E) staining

Fresh liver samples were dissected and fixed in 4% paraformaldehyde for 24 h, then embedded in paraffin. To perform H&E staining, 4 μ m liver tissue sections were stained with hematoxylin for 1 min, followed by soaking in acidic liquid alcohol differentiation for 30 s. After staining with eosin for 50 s and dehydration with ethanol (95 % and 100 %), the sections were cleared with xylene and mounted. Images were obtained using a microscope (NIKON DS-U3, Nikon, Japan) and analyzed using ImageJ software (version 2.0.0).

2.4. Masson staining and immunohistochemistry

Masson staining was performed using a Masson staining kit according to the manufacturer’s instructions (Servicebio, Wuhan, CN). After fixation for 24 h in 4% paraformaldehyde, the liver blocks were dehydrated, embedded in paraffin and cut into 4- μ m-thick slices.

For Masson staining, the slices were heated overnight at 37 °C, dewaxed and stained with Masson's dye. For immunohistochemistry, the sections were treated with blocking goat serum for 15 min, followed by overnight incubation with TGF- β 1 (1:500), Smad3 (1:500), Smad7 (1:500), TIMP-1 (1:500), MMP-2 (1:500), MMP-9 (1:500) and MMP-13 (1:200) antibodies (Servicebio, Wuhan, CN) and MMP-1 (Absin, Shanghai, CN), respectively. The sections were then treated with biotinylated-link secondary antibody and peroxidase-labeled streptavidin, followed by diaminobenzidine revelation (substrate of peroxidase) and counterstaining with Mayer's hematoxylin. The slices were analyzed under a microscope.

2.5. Immunofluorescent staining

The liver slices were rinsed with PBS for 40 min and then permeabilized with 0.3 % Triton X-100 for 10 min. Subsequently, the slices were blocked with 5% serum for 2 h at room temperature. Each liver slice was then incubated with primary antibodies at 4 °C overnight. The primary antibodies used were anti-BCL2-associated X protein (BAX) (1:400, Servicebio, Wuhan, CN) and anti-B-cell lymphoma 2 (BCL2 (1:400, Servicebio, Wuhan, CN). The sections were then rinsed with PBS for 1 h and incubated with corresponding secondary antibodies (1:200) for 1 h at room temperature. Finally, the slices were covered with 4',6-diamidino-2-phenylindole (DAPI) (Servicebio, Wuhan, CN) to stain the total nuclei. The stained sections were observed under a fluorescence microscope (Olympus BX 60 fluorescence microscope, Japan) and images were collected.

2.6. Quantitative real-time PCR (qRT-PCR)

Total RNA was isolated from the cells using TRIzol and complementary DNA was synthesized using the Invitrogen Superscript cDNA Synthesis kit (Thermo Fischer Scientific), following the manufacturer's protocol. The following primers were used:

Gene	Orientation	Sequences (5'-3')
TGF- β 1	Forward	GCAACAATTCCTGGCGTTACCTTG
	Reverse	CAGCCACTGCCGTACAACCTCC
Smad3	Forward	TTGACAGAGAGCAACACAGTAT
	Reverse	CTTCATCCAGATCGATTGCTTG
Smad7	Forward	TCGGACAGCTCAATTGGGACAAC
	Reverse	AGTGTGGCGGACTTGATGAAGATG
TIMP-1	Forward	GCATCTCTGGCATCTGGCATCC
	Reverse	CGCTGGTATAAGGTGGTCTCGTTG
MMP-1	Forward	TTCTGGTCTTCTGGCACACG
	Reverse	TTGTAGCCTTTGGAAGTCTTG
MMP-2	Forward	GATAACCTGGATGCCGTCGT
	Reverse	TGGTGTGCAGCGATGAAGAT
MMP-9	Forward	TCGTGGTTCCAACCTCGGTTT
	Reverse	GGGTGTAGAGTCTCTCGCTG
MMP-13	Forward	GAGTGATGATAATCCGGACCAT
	Reverse	CTCCTCACTGATGTTGATTCTC
BAX	Forward	TGCTAGCAAACCTGGTCTCA
	Reverse	CAGCCACCCTGGTCTTGAT
BCL2	Forward	TGGATGGCCTTTGTGGAACATA
	Reverse	CCAGGTATGCACCCAGAGTGA
β -actin	Forward	CCTGGCACCCAGCACAAAT
	Reverse	GGGCCGGACTCGTCATAC

The expression of all target genes was normalized to that of the internal control, β -actin and were quantified by the $2^{-\Delta\Delta CT}$ method.

2.7. Detection of fecal microbiome and metabolome

Mouse fecal samples were collected from the control, model and DMBG groups. The fecal samples were mixed with 10 μ L of internal standard (2-chloro-1-phenylalanine in methanol, 0.3 mg/mL) and 300 μ L of extraction solvent (methanol/water: 4/1, v/v). The extracts were centrifuged at 4 °C at 13,000 rpm for 10 min and the supernatant was dried. Then a total of 200 μ L of methanol/water (1/4; v/v) was added and the mixture was stirred for 30 s. The supernatant was analyzed by liquid chromatography–mass spectrometry using an ACQUITY UPLC system (Waters Corp., Milford, MA, USA) and QE high resolution mass spectrometer to find differential metabolites.

The total genomic DNA was extracted by DNeasy PowerSoil kit (Qiagen, Germantown, MD, USA) and then quantified by agarose gel electrophoresis. Forward (343F: 5'-TACGGRAGGCAGCAG-3') and reverse (798R: 5'-AGGGTATCTAATCTCT-3') primers were used to amplify the 16S rRNA gene region covering the V3–V4 region. The PCR products were purified by magnetic beads and used as templates in the subsequent round of PCR amplification and the concentration was measured by Qubit dsDNA analysis kit (Life Technologies Corp., Carlsbad, CA, USA). Samples were mixed according to the concentration and sequenced by computer. Finally, the correlation between the flora and metabolites were conducted by Spearman bivariate correlate analysis.

2.8. Statistical analysis

Data were analyzed using SPSS version 24 (IBM, NY, USA). All data are expressed as means \pm SD. One-way analysis of variance (ANOVA) and multiple comparison analyses were used to determine group differences, with LSD multiple comparison used when normality was detected (Shapiro-Wilk Normality Test was used to test for normality) and ANOVA-Dunnnett's T3 method used when no homogeneity was detected. Values with $P < 0.05$ were considered statistically significant.

3. Results

3.1. Metformin improved the general condition of mice

The weight of mice in both the model and metformin treatment groups decreased significantly during the first week of the experiment, followed by a gradual increase. At the end of the experiment, the body weight of the mice in both groups were significantly lower than those in the control group ($P < 0.001$). However, no significant difference in body weight was observed between the metformin and model groups (Fig. 1A and B). Compared with that in the control group, the average liver weight of mice in the model and metformin groups increased; however, the difference was not statistically significant (Fig. 1C). Compared with that in the control group, the average liver weight ratio of mice in the metformin and model groups significantly increased ($P < 0.001$); however, no

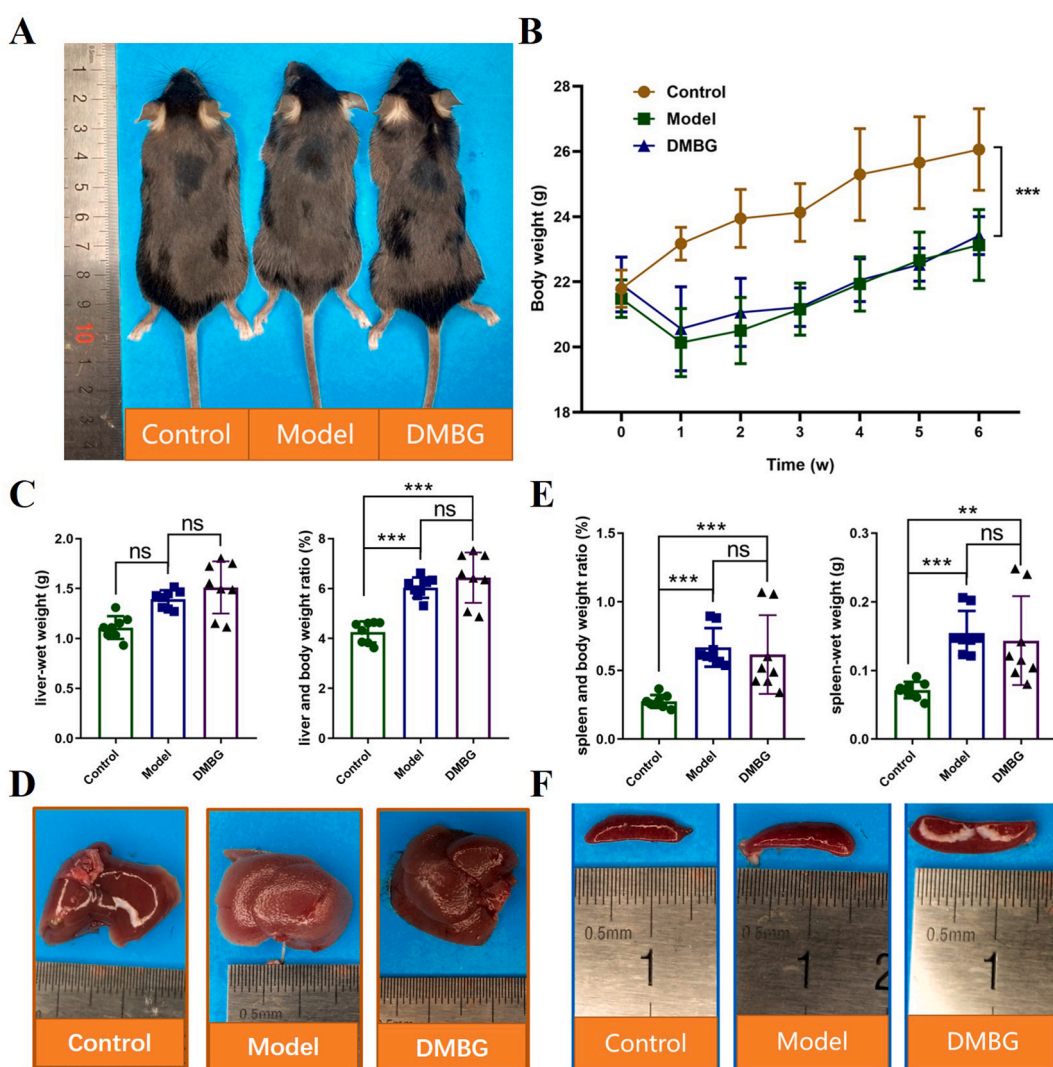


Fig. 1. Metformin improved the general condition of mice. (A) Appearance of mice in each group; (B) changes in body weight; (C) liver weight and liver/body weight ratio of mice; (D) Gross image of mouse liver; (E) spleen weight and spleen/body weight ratio of mice; (F) Gross view of mouse spleen (note: ns, no significance; * $P < 0.05$, ** $P < 0.01$, *** $P < 0.001$).

significant difference was observed between the metformin and model groups (Fig. 1C). In the control group, the liver surface was smooth, reddish-brown, soft and elastic. In contrast, in the model group, the liver surface exhibited a diffuse distribution of small nodules and the liver edge was round, shielded and adhered to the surrounding tissue. However, the livers of metformin-treated mice were smooth, had a slightly dull colour and exhibited a slightly congested surface. Nonetheless, the general appearance slightly improved compared with that of the livers in the model mice (Fig. 1D). Compared with that in the control group, the average spleen weight in both the metformin intervention and model groups was significantly higher. Simultaneously, the spleen weight ratios in both the metformin and model groups were significantly higher than that in the control group ($P < 0.001$). However, no significant difference in the spleen weight ratio was observed between the experimental and model groups (Fig. 1E and F).

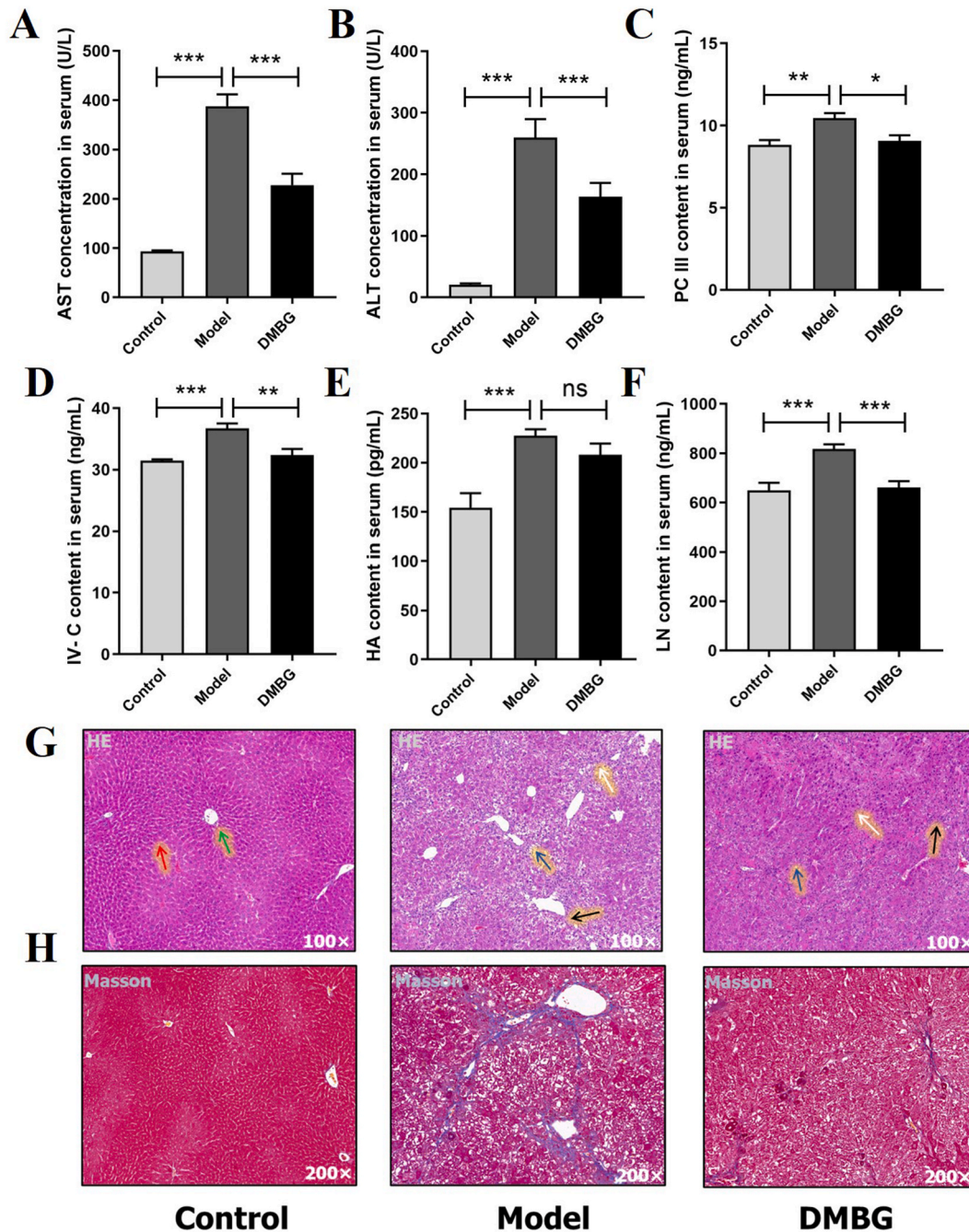


Fig. 2. Metformin improved liver function and liver fibrosis in the mice with liver fibrosis. The comparison of serum AST (A), ALT (B), PC III (C), IV-C (D), HA (E) and LN (F) levels; HE staining (H) and Masson staining (G) of liver among these groups (note: ns, no significance; * $P < 0.05$, ** $P < 0.01$ * * $P < 0.001$).

3.2. Metformin improved liver function and liver fibrosis in mice with liver fibrosis

At the end of the experiment, liver function and four parameters of liver fibrosis were examined. The results showed significant differences in the AST and ALT levels among the three groups ($P < 0.001$; Fig. 2A and B). Compared with those in the control group, the AST and ALT levels in the model group were significantly increased ($P < 0.001$). Compared with those in the model group, the AST and ALT levels in the metformin intervention group were significantly decreased ($P < 0.001$).

The results revealed statistically significant differences between the four serum markers of liver fibrosis (PC III, IV-C, HA and LN) among the three groups (Fig. 2C–F). Compared with those in the control group, the serum levels of PC III, IV-C, HA and LN in the model group were significantly increased. Compared with those in the model group, the levels of PC III, IV-C and LN in the metformin intervention group were significantly decreased. However, no significant difference in HA was observed.

We examined the liver structure using H&E staining in each group of mice. The results showed that the overall structure of liver tissue in the control group was normal, while that in the model group was abnormal. The liver cells exhibited a loosely arranged structure and a large number of liver cells showed significant oedema, with some showing vacuolar degeneration-related oedema (blue arrow). Increased abnormal fibrous connective tissue proliferation and obvious liver cirrhosis were observed. The tissue showed significant inflammatory cell infiltration (black arrows). However, the overall situation was significantly better than that in the model group. The liver cells showed a loosely arranged structure and the tissue showed mild fibrosis (white arrow, Fig. 2G). Masson's trichrome staining also revealed a significant increase in liver collagen fibres (blue) in the model group. Conversely, collagen deposition was significantly reduced in the metformin group (Fig. 2H).

3.3. Metformin inhibited inflammation and oxidative stress in mice with hepatic fibrosis

In this study, we measured the expression of liver fibrosis-related inflammatory factors and the oxidative stress index in mice with hepatic fibrosis. Variance analysis indicated significant differences in serum inflammatory indicators among the three groups ($P < 0.05$). Specifically, compared with those in the control group, the serum levels of IL-6, TNF- α and COX-2 in the model group were higher to varying degrees ($P < 0.001$, $P < 0.01$ and $P < 0.05$, respectively). In contrast, the serum levels of inflammatory markers in the metformin group were lower than those in the model group, although the difference was not statistically significant (Fig. 3A–C).

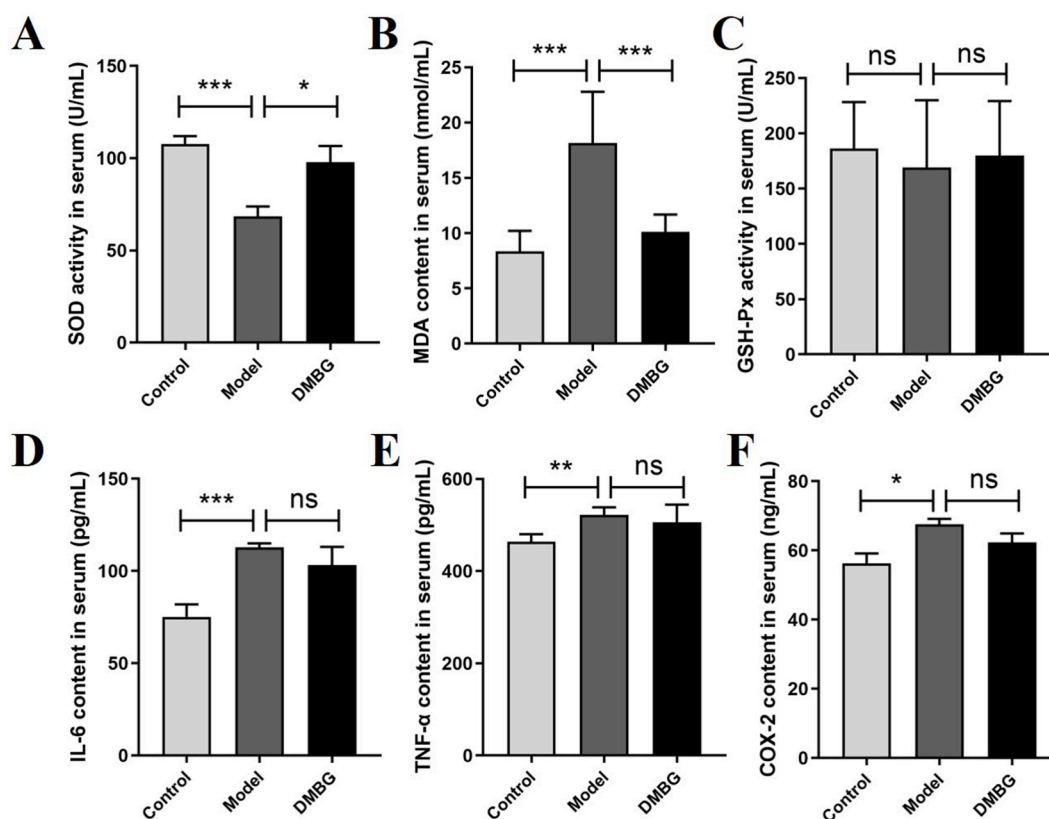


Fig. 3. Metformin inhibited inflammation and oxidative stress in mice with hepatic fibrosis. (A) Serum IL-6 levels of mice in the three groups; (B) Serum TNF- α levels in the three groups; (C) Serum COX-2 levels in the three groups of mice; (D) Serum SOD levels in the three groups; (E) Serum MDA levels in the three groups; (F) Serum GSH-Px levels of the three groups of mice (note: ns, no significance; * $P < 0.05$, ** $P < 0.01$ *** $P < 0.001$).

Moreover, it was observed that the serum SOD levels in the model group were significantly decreased ($P < 0.001$) and the MDA content was significantly increased ($P < 0.001$) compared with those in the control group. However, in the metformin group, serum SOD levels were significantly increased and MDA was significantly decreased compared with those in the model group ($P < 0.05$ and $P < 0.001$, respectively, Fig. 3D–F).

3.4. Metformin inhibited liver cell apoptosis in mice with hepatic fibrosis

Hepatocyte apoptosis is a major pathological cause of liver fibrosis. B-cell lymphoma 2 (BCL2) and BCL2-associated X protein (BAX) are the most important anti-apoptotic and apoptosis-promoting proteins, respectively, in the BCL2 family. In this study, BAX and BCL2 were analyzed for their mRNA and protein expression in the liver. The results showed that the expression of BAX mRNA in the liver of mice in the model group was significantly increased ($P < 0.001$). The expression level of BAX mRNA in the liver in the metformin-treated group was significantly lower than that in the model group (Fig. 4A). Double immunofluorescence labelling showed that the expression level of the BAX protein was consistent with its mRNA level (Fig. 4C). No significant differences in BCL2 mRNA and protein expression were observed between the model and control groups. The expression of BCL2 in the metformin treatment group was significantly increased ($P < 0.001$, Fig. 4B and C).

3.5. Effects of metformin on TGF- β /smads signalling pathway

Increased mRNA and protein expressions of the TGF- β /Smads signalling pathway in the mouse liver were detected using qPCR and immunohistochemistry. The results showed that the expression level of Smad3 mRNA in the liver in the model group was not

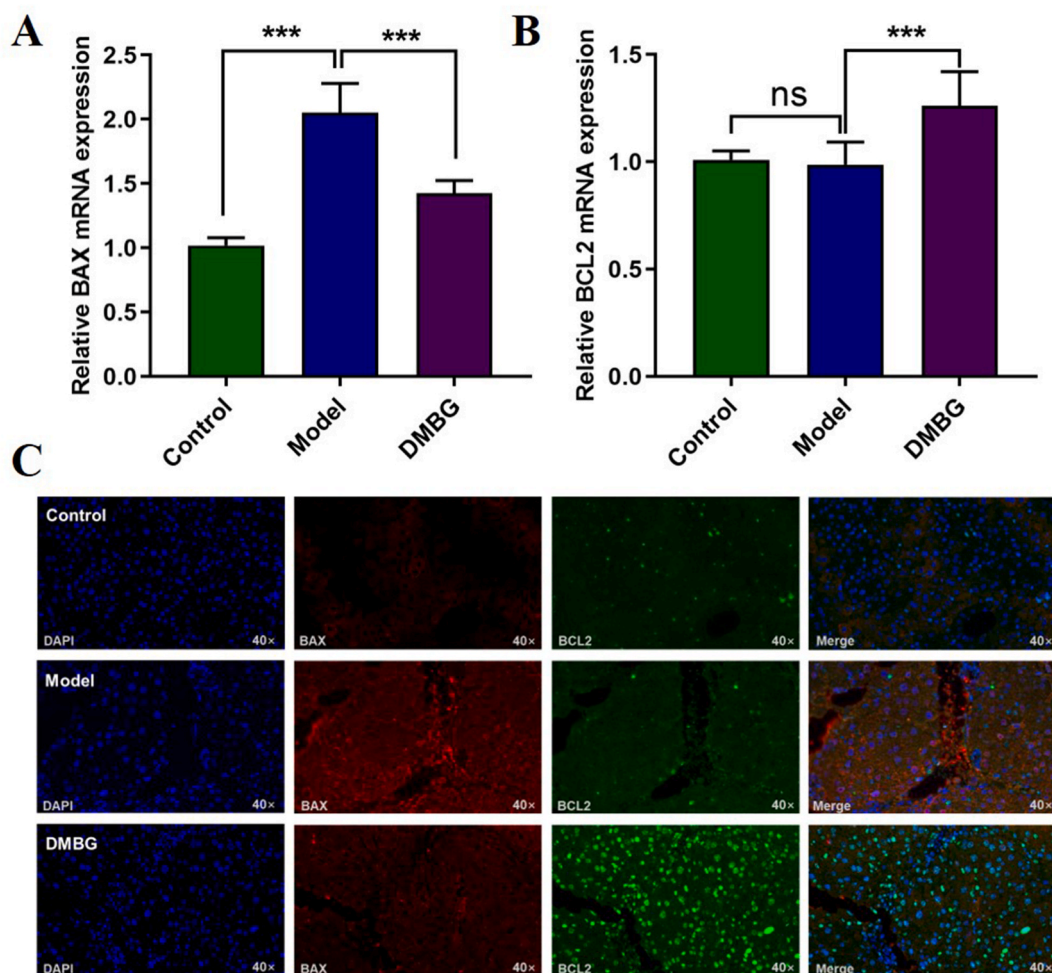


Fig. 4. Metformin inhibited liver cell apoptosis in mice with hepatic fibrosis. (A) BAX gene expression in mouse liver; (B) BCL2 expression in mouse liver; (C) Immunofluorescence was used to detect the protein expression of BAX and BCL2 in mouse liver (note: ns, no significance; * * * $P < 0.001$).

significantly different from that in the other two groups (Fig. 5A). However, the protein expression of Smad3 was significantly higher than that in the control group and the protein expression of Smad3 in the metformin group was lower than that in the model group (Fig. 5B). Compared with those in the control group, the expression levels of Smad7 mRNA and protein in the liver in the model group were significantly decreased ($P < 0.001$). In contrast, the expression levels of Smad7 mRNA and protein in the metformin group were significantly higher than those in the model group ($P < 0.001$, Fig. 5C and D). In addition, TGF- β 1 mRNA and protein expression levels in the model group were significantly increased ($P < 0.001$); however, they were significantly lower in the metformin group than in the model group ($P < 0.01$, Fig. 5E and F).

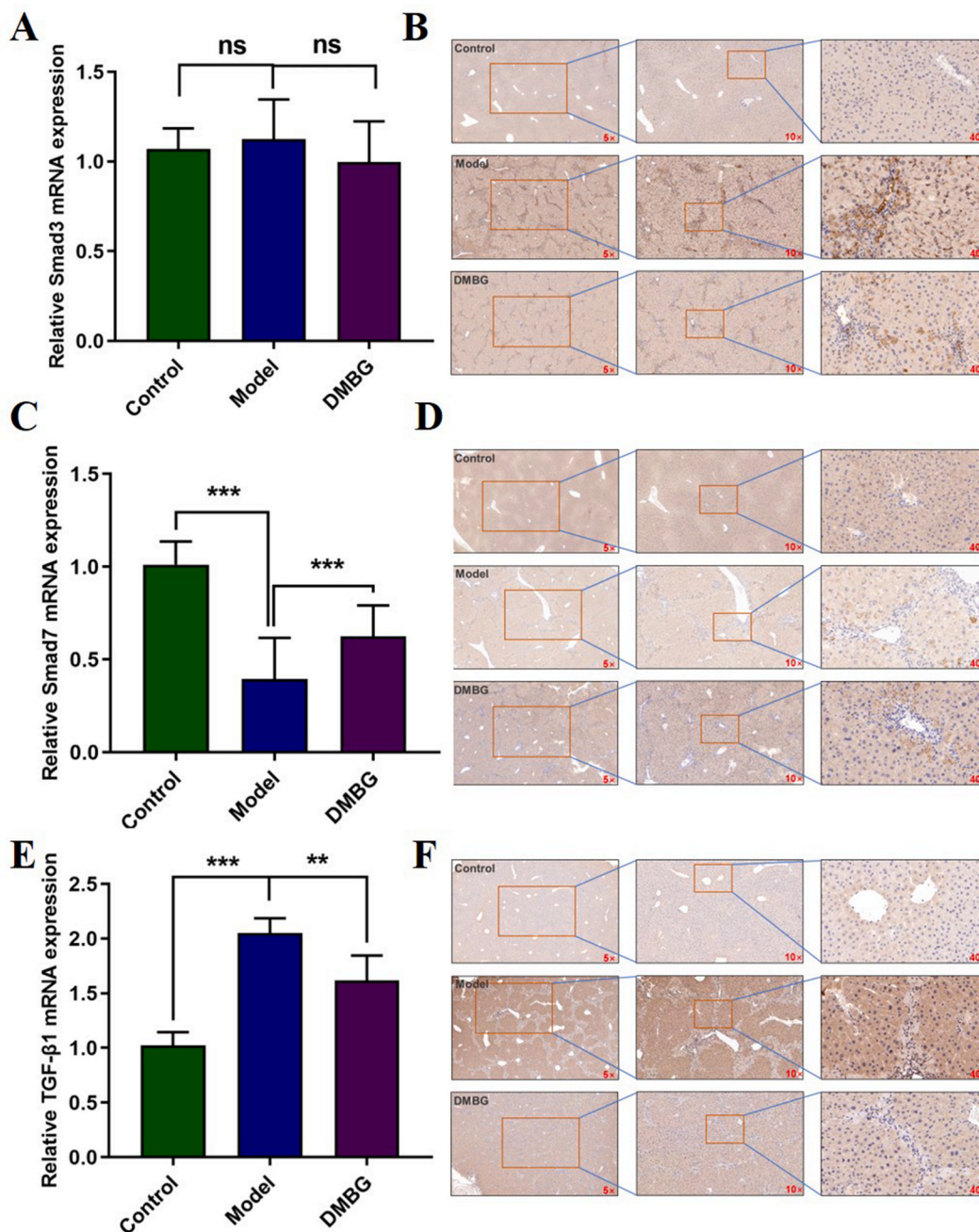


Fig. 5. Effects of metformin on TGF- β /Smads signalling pathway. The mRNA (A) and protein (B) expression of Smad3 in mouse liver; The mRNA (C) and protein (D) expression of Smad7 in mouse liver; The mRNA (E) and protein (F) expression of TGF- β in mouse liver (note: ns, no significance; ** $P < 0.01$ * * $P < 0.001$).

3.6. Effects of metformin on TIMP-1/MMPs signalling pathway

In this study, the effects of metformin on the TIMP-1/MMPs signalling pathway in the mouse liver were investigated. Our results showed that the mRNA and protein expression levels of MMP-1 and MMP-2 were significantly lower in the model group than in the control group ($P < 0.01$ and $P < 0.001$, respectively; Fig. 6A, B and F). Furthermore, the mRNA and protein expression levels of MMP-1 and MMP-2 in the metformin group were significantly higher than those in the model group ($P < 0.05$ and $P < 0.001$, respectively). However, no significant differences in the mRNA and protein expression levels of MMP-9 and MMP-13 were observed among the three groups (Fig. 6C, D and F). Furthermore, compared with those in the control group, the expression levels of TIMP-1 mRNA and protein were significantly increased in the model group ($P < 0.001$); however, they were significantly lower in the metformin group than in the model group ($P < 0.01$, Fig. 6E and F).

3.7. Analysis of differences in intestinal flora

The top 15 most abundant bacterial groups were then identified by performing a genus-level abundance analysis based on the bacterial colonies: *Muribaculaceae*, *Lachnospiraceae* NK4A136, *Alistipes*, *Rikenellaceae* RC9 gut, *Prevotellaceae* NK3B31, *Alloprevotella*, *Bacteroides*, *Clostridium* UCG-014, *Lactobacillus*, *Odoribacter*, *Helicobacter*, *Prevotellaceae* UCG-001, *Parabacteroides*, *Rikenella* (*Rikenella* spp.) and *Colidextribacter* (Fig. 7A). Subsequently, we performed a differential flora analysis. The results revealed that 27 bacterial genera were significantly different between the groups (Fig. 7B and Table S1). The top ten genera were *Muribaculaceae*, *Rikenellaceae* RC9 gut group, *Bacteroides*, *Odoribacter*, *Helicobacter*, *Parabacteroides*, *Parabacteroides*, *Rikenella*, *Clostridia* vadin BB60 group, *Parasutterella* and *Eubacterium ruminantium*. Metformin significantly ameliorated *Bacteroides*, *Helicobacter*, *Parabacteroides*, *Clostridia* vadin BB60 group and *Parasutterella*, making the intestinal flora more similar to that of control mice. These findings suggest that metformin may play a role in modulating the intestinal microbiota, particularly by affecting these key genera.

3.8. Comparison of intestinal differential metabolites in mice in each group

The differential metabolites between the model and control groups were analyzed and the results showed that 481 metabolites were significantly different between the two groups. Fig. 8A and Table S2 show the top 50 differential metabolites, including

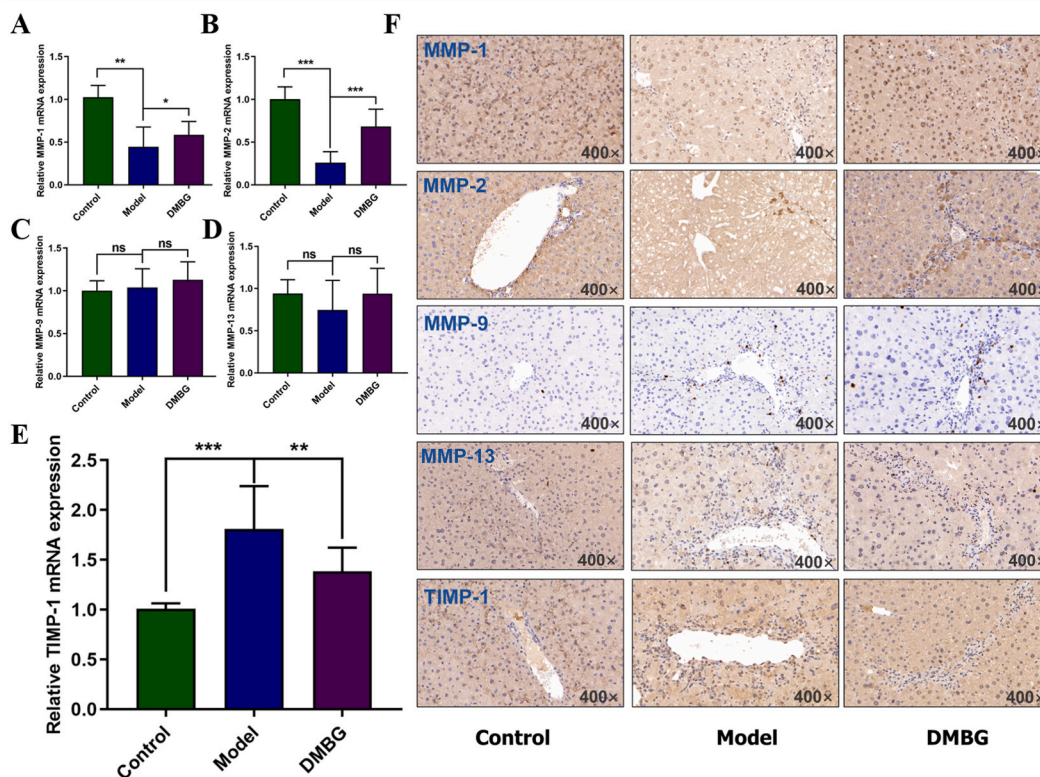


Fig. 6. Effects of metformin on TIMP-1/MMPs signalling pathway. The mRNA expression of MMP-1(A), MMP-2 (B), MMP-9 (C), MMP-13 (D) and TIMP-1 (E) in the liver of the mice; (F) The protein expression of these TIMP-1 and MMPs (note: ns, no significance; *P < 0.05, **P < 0.01, ***P < 0.001).

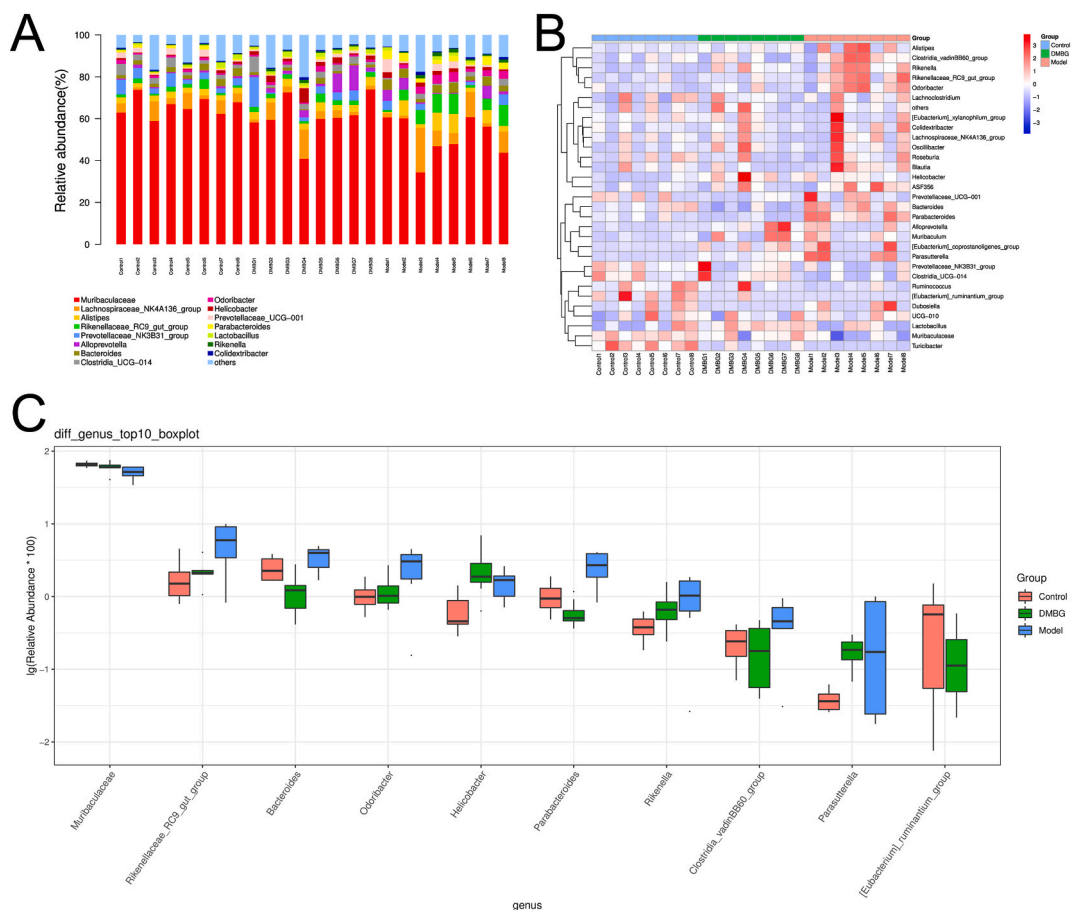


Fig. 7. Difference analysis of intestinal flora. (A) Histogram of TOP15 flora abundance ranking; (B) Heat maps of different flora in each group; (C) TOP10 different flora.

laurylaldehyde, capsidiol, omega-hydroxy myristic acid, tridecanoic acid, docosahexaenoylcholine, myristamide, 3-carboxamide, convolvulinic acid, 17-alpha-ethinyl oestradiol and docosahexaenoylcholine. We compared the differential metabolites between the metformin and model groups and identified 385 statistically different differential metabolites. Further the results showed the top 50 differential metabolites, including helvolic acid, ethyl isovalerate, ipurolic acid, ganoderic acid L, physalolactone B, 2-decylfuran, 3-oxododecanoic acid glycerides, trigonelline, dihydroartemisinin and cucurbitacin E (Fig. 8C and Table S3).

3.9. Enrichment analysis of metabolic pathways

After identifying the differential metabolites between the groups, the differential metabolites were analyzed using the KEGG database for metabolic pathway analysis (<https://www.kegg.jp>). As shown in Fig. 9A and B, the top 20 metabolic pathways and the top 8 metabolic enrichment pathways are shown in bubble maps, with significant differences between the model and control groups. These pathways include purine metabolism, caffeine metabolism, carbohydrate digestion and absorption, pyrimidine metabolism, bile secretion, ABC transport and pentose and glucuronic acid interconversion. As can be seen in Fig. 9C and D, there are significant differences between groups of metformin and model users with respect to the top 20 metabolic pathway bubble maps as well as the top thirteen metabolic enrichment pathways. These pathways include purine metabolism, linoleic acid metabolism, regulation of adipocyte lipolysis, neuroactive ligand-receptor interaction, arachidonic acid metabolism, renin secretion, PPAR signalling pathway, arginine biosynthesis and cAMP signalling pathway.

3.10. Association analysis of intestinal flora and metabolites

After obtaining the differential flora and metabolites, Spearman correlation analysis was performed on the top 20 flora and metabolites with the most significant differences. The results revealed potential regulatory relationships between the flora and metabolites in the model and control groups (Fig. 10A and B). Further analysis and screening identified microbiota-metabolite pairs with potential regulatory effects. For instance, the *Turicibacter* genus was positively correlated with metabolites such as 7-sulfonic acid,

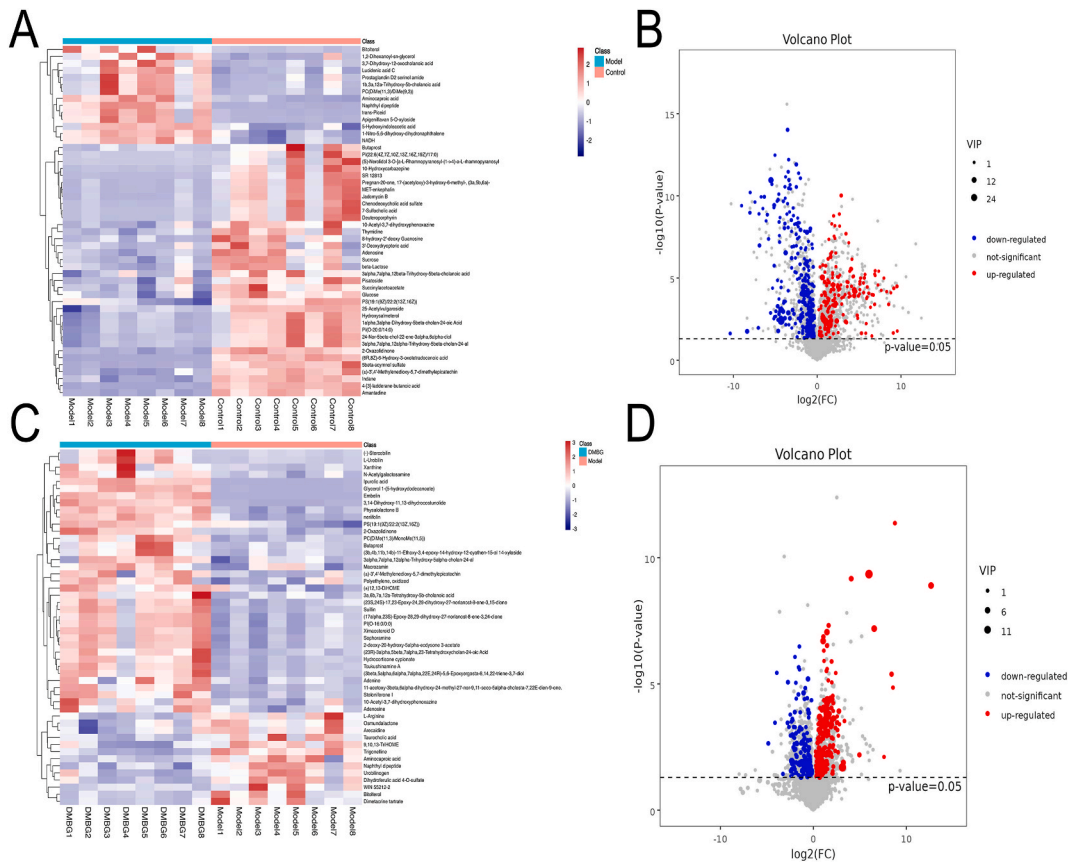


Fig. 8. Comparison of intestinal differential metabolites in mice of each group. (A) Heat map of TOP50 differential metabolites between the model group and the control group; (B) Volcano map of differential metabolites between model group and control group; (C) Heat map of TOP50 differential metabolites between metformin group and model group; (D) Volcano plot of differential metabolites in metformin group and model group.

porphyrin, succinic acid and 2-oxazolidinone, which were reduced in the model group. The abundance of *Helicobacter* increased in the model group and negatively correlated with a decrease in 2-oxazolidinone content. *Lachnospiraceae* UCG-006 positively correlated with 5-hydroxyindoleacetic acid levels, which were significantly higher in the model group (Table 1). We further analyzed the relationship between changes in the microbiota and their metabolites after metformin intervention in the treatment of liver fibrosis (Fig. 10C and D, Table 2). *Candidatus* Arthromitus was significantly reduced in the metformin group and a positive correlation was observed between the metabolites naphthal dipeptide, aminoacetic acid, 2-oxazolidinone and others. In addition, Bacteroidetes negatively correlated with 2-oxazolidinone, sacrophanic acid and plantolactone B. Moreover, Spearman bivariate correlation analysis indicated that *Prevotella* abundance was significantly decreased in the metformin group and positively correlated with decreased taurocholic acid levels.

4. Discussion

Liver fibrosis is a pathological process that occurs during the development of chronic liver disease, leading to the formation of liver lesions due to long-term stimulation. Several studies have shown that the liver has a robust regenerative function and that liver fibrosis is not a unidirectional progressive process [12]. Thus, the timely removal of stimulating factors and appropriate interventions can reverse liver fibrosis.

Metformin has been shown to exert synergistic effects on multiple targets, including inflammation, oxidative stress, apoptosis and signalling pathway regulation [9]. The hepatic fibrosis test is mainly used to diagnose the development of chronic liver disease, assess its therapeutic effects and measure the degree of inflammatory activity and fibrosis. We found that metformin improved liver function and reduced the serum levels of PC III, IV-C, HA and LN (Fig. 2C–F). Furthermore, H&E and Masson’s trichrome staining indicated that metformin significantly inhibited liver fibrosis (Fig. 2G and H). The potential mechanism of action of metformin in hepatic fibrosis, focusing on inflammation, oxidative stress, apoptosis and pathway regulation was evaluated.

In hepatocytes, reactive oxygen species (ROS) are mainly produced in the electron transport chain of the mitochondria and during protein folding [13,14], which can significantly activate the expression of hepatic stellate cells (HSC) and further increase ECM

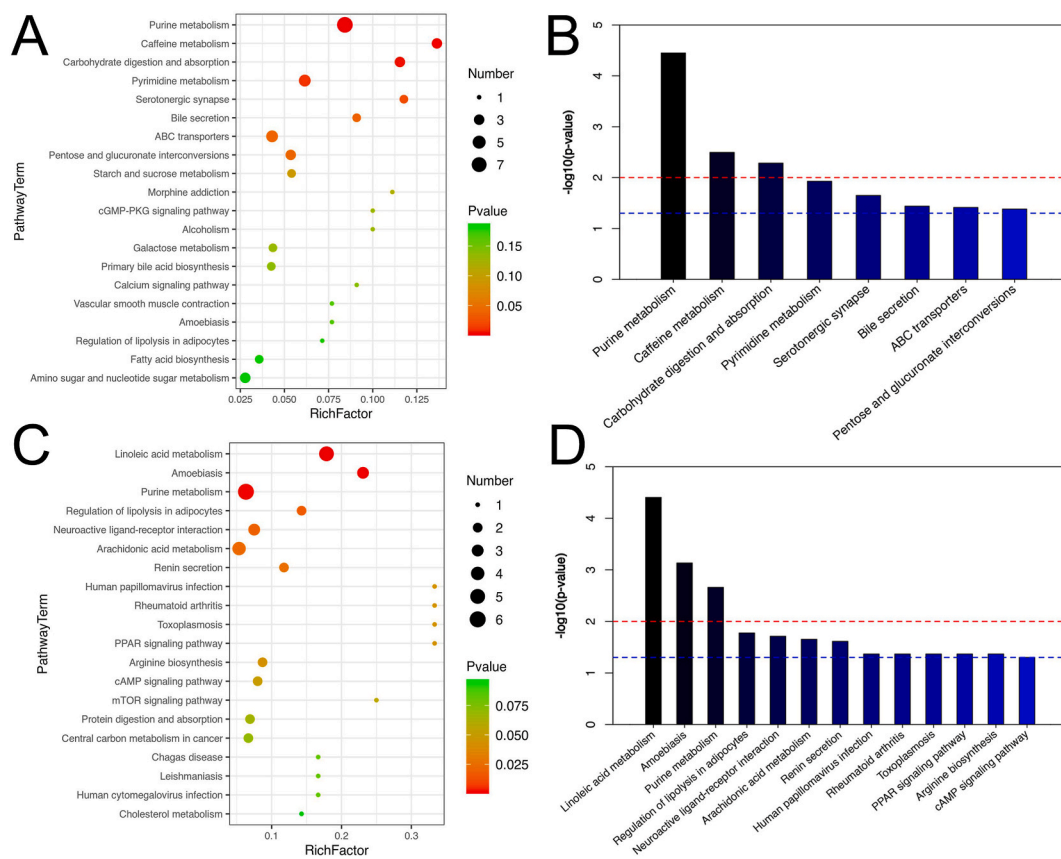


Fig. 9. Enrichment analysis of metabolic pathways. (A) The enrichment bubble map of TOP20 metabolic pathway in the model group and the control group; (B) enrichment map of differential metabolic pathways between the model group and the control group; (C) Enrichment bubble map of TOP20 metabolic pathway in metformin group and model group; (D) Enrichment map of differential metabolic pathways in metformin group and model group.

production. In this study, the serum levels of MDA, SOD and GSH-Px in mice were measured. The results showed that metformin inhibited the expression of MDA and increased the expression of SOD but had no significant effect on GSH-Px. This suggested that metformin plays a role in the regulation of oxidation-antioxidant homeostasis during liver fibrosis. It has been widely confirmed that metformin can reduce oxidative stress by regulating the redox state of hepatocytes, thereby further developing chronic liver diseases, such as nonalcoholic fatty liver disease and chronic hepatitis, into liver fibrosis, cirrhosis and even liver cancer [15]. Metformin also promotes the activation of nuclear factor erythroid 2-related factor 2 (NRF2), a major regulator of oxidative stress, in various animal models of liver disease [16–18]. Therefore, metformin benefits the activation of NRF2 and regulation of oxidative stress in the treatment of chronic liver diseases.

Inflammatory cytokines play important roles in the development of liver fibrosis. A positive feedback pathway has been established between fibrotic cells and inflammatory cells [19,20]. Studies have shown that the loss of macrophages can reduce fibrogenesis and scar formation in a CCl₄-induced liver fibrosis mouse model, suggesting that macrophages play an essential role in promoting liver fibrosis [21]. It was observed that the levels of the cytokines IL-6, TNF- α and COX-2 increased to varying degrees in the liver fibrosis mouse model. Metformin inhibits the expression of these cytokines to a certain extent. *In vitro* studies demonstrated that metformin inhibited the activation of NK- κ B by targeting the protein kinase B (PKB) and extracellular regulated kinase 1/2 (ERK1/2) signalling pathways. This action reduced the secretion of IL-6 and IL-8 induced by IL-1 β in endothelial cells, vascular smooth muscle cells and macrophages, thereby exerting anti-inflammatory effects [8,22]. However, this study was limited by its small sample size and substantial differences within the groups. Although metformin did not significantly reduce the expression of related pro-inflammatory factors, an overall downward trend was observed, suggesting an anti-inflammatory effect of metformin on liver fibrosis to a certain extent.

Apoptosis of liver cells can stimulate the production of HSC in various ways, including the production of inflammatory cytokines, thus accelerating the progression and deterioration of liver diseases [23]. In the present study, it was observed that metformin inhibited hepatocyte apoptosis in mice with liver fibrosis. A dynamic evolutionary process of the two factors plays an important role in preventing the progression of liver fibrosis [24,25]. Thus, active inhibition of hepatocyte apoptosis and promotion of HSC apoptosis can effectively reverse liver fibrosis.

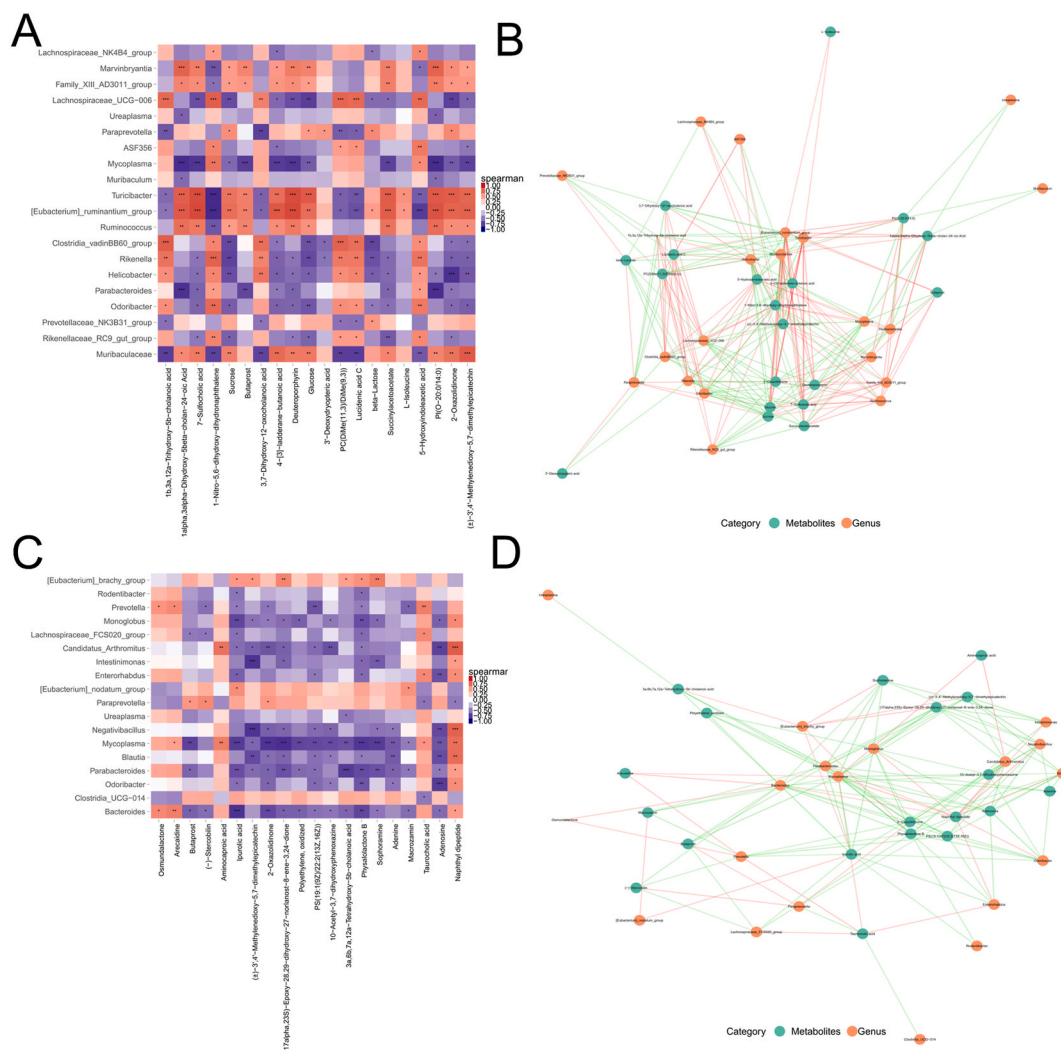


Fig. 10. Association analysis of intestinal flora and metabolites. (A) Heat map of TOP20 differential flora and metabolite correlation between the model group and the control group; (B) TOP20 differential flora and metabolite association network between the model group and the control group; (C) Heat map of TOP20 differential flora and metabolites between metformin group and model group; (D) Association network of TOP20 differential flora and metabolites between metformin group and model group.

Studies indicated on the signalling pathways closely related to the occurrence and development of liver fibrosis has garnered substantial interest. Studies indicate that the activation and proliferation of HSC are closely related to the TGF- β /Smads pathway. TGF- β is implicated in the progression of liver diseases, from injury and inflammation to fibrosis, cirrhosis and even liver cancer [26,27]. TGF- β /Smads signalling pathway is the main pathway through which TGF- β exerts its biological effects. In addition, ECM secretion is directly influenced by the TIMP-1/MMPs pathway [28]. The results of this study demonstrate that metformin inhibited the expression of TGF- β 1 and promoted the expression of Smad7 but had no significant effect on Smad3. Nikolettta et al. [29] found that TGF- β /Smad7 was activated in patients with chronic hepatitis B fibrosis. TGF- β was highly expressed in patients with liver fibrosis, while Smad7 was significantly inhibited. We also found that TIMP-1 levels decreased significantly after metformin treatment, accompanied by an increase in MMP-1 and MMP-2 levels. As a physiological MMP inhibitor, TIMP-1 can significantly inhibit MMP activity, thereby inhibiting ECM degradation. Therefore, an imbalance between TIMP-1 and MMPs leads to increased ECM synthesis and decreased ECM degradation, resulting in liver fibrosis. These findings suggested that metformin may play an anti-fibrotic role through the TGF- β /Smads and TIMP-1/MMPs pathways.

With the advancement of gut microbiota research and the development of metabolomic technology, researchers have paid increasing attention to the role of the gut microbiota and its metabolites in diseases and their treatment. One particularly significant bidirectional pathway is the “gut-liver axis”, which is vital due to its congenital developmental advantages. The “gut-liver axis” was initially proposed in 1978 and has since attracted considerable attention. Any factor that affects intestinal flora metabolism may impact disease development and progression. Based on the “gut-liver axis” theory, this study analyzed changes in the gut microbiota

Table 1

Potential significance of intestinal microbiota - metabolite regulation in the development of liver fibrosis.

metabolites	Genus	Correlation	P value	AdjPvalue
7-Sulfocholic acid	Turicibacter	0.891526	6.37E-06	5.32E-05
Deuteroporphyrin	Turicibacter	0.874172	9.54E-06	8.52E-05
Glucose	Turicibacter	0.809419	0.000146	0.000582
Succinylacetoacetate	Turicibacter	0.802061	0.000186	0.000619
2-Oxazolidinone	Turicibacter	0.796174	0.000224	0.000641
2-Oxazolidinone	Helicobacter	-0.8	0.000305	0.006091
Lucidenic acid C	Lachnospiraceae_UCG-006	0.761765	0.000926	0.004283
Lucidenic acid C	Muribaculaceae	-0.75294	0.001147	0.005256
5-Hydroxyindoleacetic acid	Lachnospiraceae_UCG-006	0.75	0.001228	0.004283
2-Oxazolidinone	Lachnospiraceae_UCG-006	-0.74118	0.001499	0.004283
Succinylacetoacetate	Ruminococcus	0.712289	0.001962	0.013058
Lucidenic acid C	Clostridia_vadinBB60_group	0.726471	0.002048	0.009223
Sucrose	Rikenella	-0.72353	0.002174	0.012936
beta-Lactose	Clostridia_vadinBB60_group	-0.72059	0.002306	0.009223
Sucrose	Turicibacter	0.701987	0.002434	0.004426
2-Oxazolidinone	Muribaculaceae	0.717647	0.002444	0.00611
Butaprost	Parabacteroides	-0.71765	0.002444	0.016293
5-Hydroxyindoleacetic acid	Rikenella	0.702941	0.003234	0.012936
Sucrose	Clostridia_vadinBB60_group	-0.70294	0.003234	0.01078
7-Sulfocholic acid	Ruminococcus	0.68727	0.003265	0.013058

Table 2

Potential microbiota-metabolite regulation relationship of metformin against hepatic fibrosis.

metabolites	Genus	Correlation	P value	AdjPvalue
Naphthyl dipeptide	Candidatus_Arthromitus	0.807013636	0.000158	0.003156
Ipuolic acid	Bacteroides	-0.797058824	0.000337	0.006738
Naphthyl dipeptide	Negativibacillus	0.782352941	0.000533	0.005334
Adenosine	Odoribacter	-0.764705882	0.00086	0.01721
Naphthyl dipeptide	Blautia	0.740416201	0.001037	0.019368
Adenosine	Candidatus_Arthromitus	-0.732470208	0.001252	0.012515
Aminocaproic acid	Candidatus_Arthromitus	0.709783077	0.002069	0.013796
Physalolactone B	Bacteroides	-0.714705882	0.002588	0.019315
2-Oxazolidinone	Bacteroides	-0.708823529	0.002897	0.019315
Adenosine	Blautia	-0.693218355	0.002905	0.019368
Physalolactone B	Parabacteroides	-0.705882353	0.003062	0.023301
Adenosine	Negativibacillus	-0.702941176	0.003234	0.021559
Physalolactone B	Monoglobus	-0.687095947	0.003276	0.032756
Sophoramine	[Eubacterium]_brachy_group	0.676184914	0.00403	0.080593
Ipuolic acid	Parabacteroides	-0.685294118	0.004431	0.023301
Taurocholic acid	Prevotella	0.662879922	0.005131	0.051314
Adenosine	Enterorhabdus	-0.676470588	0.005147	0.090939
2-Oxazolidinone	Candidatus_Arthromitus	-0.661167798	0.005289	0.021157
Sophoramine	Parabacteroides	-0.667647059	0.005951	0.023806
Physalolactone B	Odoribacter	-0.658823529	0.006852	0.068521

and its metabolites during metformin intervention. We found that metformin significantly increased the abundance of *Bacteroides*, *Parabacteroides* and *Clostridia vadin BB60 group*, while decreasing the abundance of *Parasutterella* and *Helicobacter*. This change made the flora more similar to that of the control mice. A study on the intestinal flora of 217 Hispanic participants revealed a reduced abundance of *Bacteroides* and *Parabacteroides* in the intestinal flora of individuals with liver fibrosis [30]. Another previous study also found that *Helicobacter* infection leads to liver fibrosis in mice by activating the inflammatory response and enhancing oxidative stress [31,32]. *Clostridium* plays essential roles in metabolism, improving immunity and preventing the invasion of pathogenic bacteria [33]. Metformin can inhibit the imbalance of the above-mentioned bacteria, induced by CCl₄ and exhibit anti-fibrotic effects. One way metformin exerts this effect may involve regulating bacterial flora or inhibiting the secretion of certain metabolites. Our findings indicated that metformin intervention significantly reduced the abundance of *Prevotella* and this reduction was significantly positively correlated with reduced taurocholate (TCA) levels. Cholestasis is a crucial pathological change in the progression of liver fibrosis to cirrhosis and TCA levels significantly increase during this process [34]. Both domestic and foreign studies have suggested that high TCA levels can act on hepatocytes via the “enterohepatic axis” to accelerate the progression of liver cirrhosis. Therefore, TCA may become a potential target for the clinical treatment of liver cirrhosis in the future [35]. There are various ways in which TCA promotes liver cirrhosis. Numerous studies have shown that TCA can enhance toll-like receptor 4 (TLR4) expression in HSC and activate TGF- β -dependent HSC to promote liver fibrosis progression [36,37]. Therefore, TCA plays an important role in promoting the development of liver fibrosis. *Prevotella* is a Gram-negative immunocommensal bacterium comprising more than 50 species. It helps the body break down proteins and carbohydrates and acts as an opportunistic pathogen that causes inflammatory diseases in the body.

In this study, a positive correlation was found between bacterial flora and TCA content. Consistent with the results of this study, recent studies have reported a significant increase in *Prevotella* abundance during liver fibrosis [30].

The present study revealed that metformin has anti-fibrotic effects in the liver and the mechanism needs to be further verified experimentally. In addition, large-sample clinical studies are warranted to evaluate changes in the differential flora and metabolites in the clinical population. However, the establishment of a risk prediction model for liver fibrosis progression based on flora and metabolites could better translate these results and provide a theoretical basis for the use of metformin in clinical anti-liver fibrosis treatment.

5. Conclusions

Metformin can improve the general condition and liver function of mice and also inhibit liver fibrosis in mice induced by CCl₄. The anti-hepatic fibrosis mechanism of metformin is multifaceted, encompassing anti-inflammatory, anti-oxidative stress injury, hepatocyte apoptosis inhibition, regulation of the TGF- β /Smad7 and TIMP-1/MMPs signalling pathways, as well as other effects. The intestinal flora and its metabolites also play pivotal roles in this process. Metformin significantly ameliorated the imbalance of *Bacteroides*, *Helicobacter*, *Parabacteroides*, *Parasutterella* and so on, making the intestinal flora more similar to that of control mice. 385 differential metabolites were identified between the metformin and model groups, including helvolic acid, ethyl isovalerate, ipurolic acid, ganoderic acid L, physalolactone B, 2-decylfuran, 3-oxododecanoic acid glycerides, trigonelline, dihydroartemisinin and cucurbitacin E. The metabolic pathways involved include purine metabolism, linoleic acid metabolism, regulation of adipocyte lipolysis, neuroactive ligand-receptor interaction, arachidonic acid metabolism, renin secretion, PPAR signalling pathway, arginine biosynthesis, and cAMP signalling pathway. Among which, *Prevotella* abundance significantly decreased in the metformin group and positively correlated with decreased taurocholic acid levels. Spearman bivariate correlation analysis indicates that *Prevotella* abundance was significantly decreased in the metformin group and positively correlated with decreased taurocholic acid levels, which indicates that Metformin may play an anti-fibrosis role by inhibiting *Prevotella* and reducing taurocholic acid secretion. This potential regulatory network requires further experimental verification.

Funding

This study was supported by grants from National Science and Technology Major Project to Jun Li (No. 2017ZX10203202-002-005), the Science and Technology Development Foundation Project of the Affiliated Hospital of Xuzhou Medical University [No. XYFM2021049] and the Natural Science Research Project of Huai'an City (No. HAB202318 and HABZ202202) to Jie Zhang.

Data availability statement

The datasets of 16s and LC-MS for this study can be found in the "Baidu Netdisk" (https://pan.baidu.com/s/1_hYIhuSsqQn2ZxVPxs6h2A?pwd=fp12) with the extraction code fp12.

CRedit authorship contribution statement

Lianhua Kong: Writing – original draft, Validation. **Juncong Ma:** Writing – original draft, Data curation. **Li Dong:** Software, Resources, Data curation. **Chuanlong Zhu:** Software, Data curation. **Jie Zhang:** Writing – review & editing, Project administration, Conceptualization. **Jun Li:** Writing – review & editing, Supervision, Project administration.

Declaration of competing interest

The authors declare that they have no known competing financial interests or personal relationships that could have appeared to influence the work reported in this paper.

Acknowledgments

Not applicable.

Appendix A. Supplementary data

Supplementary data to this article can be found online at <https://doi.org/10.1016/j.heliyon.2024.e24610>.

References

- [1] M. Parola, M. Pinzani, Liver fibrosis: pathophysiology, pathogenetic targets and clinical issues, *Mol. Aspect. Med.* 65 (2019) 37–55. <https://doi.org/10.1016/j.mam.2018.09.002>.

- [2] A. Baiocchini, C. Montaldo, A. Conigliaro, A. Grimaldi, V. Correani, F. Mura, F. Ciccocanti, N. Rotiroli, A. Brenna, M. Montalbano, G. D'Offizi, M.R. Capobianchi, R. Alessandro, M. Piacentini, M.E. Schininà, B. Maras, F. Del Nonno, M. Tripodi, C. Mancone, Extracellular matrix molecular remodeling in human liver fibrosis evolution, *PLoS One* 11 (3) (2016) e0151736. <https://doi:10.1371/journal.pone.0151736>.
- [3] L. Campana, J.P. Iredale, Regression of liver fibrosis, *Semin. Liver Dis.* 37 (1) (2017) 1–10. <https://doi:10.1055/s-0036-1597816>.
- [4] R.C. Shankarajah, E. Callegari, P. Guerriero, A. Rimessi, P. Pinton, L. Gramantieri, E.M. Silini, S. Sabbioni, M. Negrini, Metformin prevents liver tumorigenesis by attenuating fibrosis in a transgenic mouse model of hepatocellular carcinoma, *Oncogene* 38 (45) (2019) 7035–7045. <https://doi:10.1038/s41388-019-0942-z>.
- [5] V. Kheirollahi, R.M. Wasnick, V. Biasin, A.I. Vazquez-Armenariz, X. Chu, A. Moiseenko, A. Weiss, J. Wilhelm, J.S. Zhang, G. Kwapiszewska, S. Herold, R. T. Schermuly, B. Mari, X. Li, W. Seeger, A. Günther, S. Bellusci, E. El Agha, Metformin induces lipogenic differentiation in myofibroblasts to reverse lung fibrosis, *Nat. Commun.* 10 (1) (2019) 2987. <https://doi:10.1038/s41467-019-10839-0>.
- [6] M. Wu, H. Xu, J. Liu, X. Tan, S. Wan, M. Guo, Y. Long, Y. Xu, Metformin and fibrosis: a review of existing evidence and mechanisms, *J. Diabetes Res.* 2021 (2021) 6673525. <https://doi:10.1155/2021/6673525>.
- [7] S. Verdura, E. Cuyàs, B. Martin-Castillo, J.A. Menendez, Metformin as an archetype immuno-metabolic adjuvant for cancer immunotherapy, *OncoImmunology* 8 (10) (2019) e1633235. <https://doi:10.1080/2162402x.2019.1633235>.
- [8] K. Isoda, J.L. Young, A. Zirlík, L.A. MacFarlane, N. Tsuboi, N. Gerdes, U. Schönbeck, P. Libby, Metformin inhibits proinflammatory responses and nuclear factor- κ B in human vascular wall cells, *Arterioscler. Thromb. Vasc. Biol.* 26 (3) (2006) 611–617. <https://doi:10.1161/01.Atrv.0000201938.78044.75>.
- [9] G. Rena, D.G. Hardie, E.R. Pearson, The mechanisms of action of metformin, *Diabetologia* 60 (9) (2017) 1577–1585. <https://doi:10.1007/s00125-017-4342-z>.
- [10] Y. Chen, F. Yang, H. Lu, B. Wang, Y. Chen, D. Lei, Y. Wang, B. Zhu, L. Li, Characterization of fecal microbial communities in patients with liver cirrhosis, *Hepatology* 54 (2) (2011) 562–572. <https://doi:10.1002/hep.24423>.
- [11] H. Fukui, Leaky gut and gut-liver Axis in liver cirrhosis: clinical studies update, *Gut Liver* 15 (5) (2021) 666–676. <https://doi:10.5009/gnl20032>.
- [12] T. Kisseleva, D. Brenner, Molecular and cellular mechanisms of liver fibrosis and its regression, *Nat. Rev. Gastroenterol. Hepatol.* 18 (3) (2021) 151–166. <https://doi:10.1038/s41575-020-00372-7>.
- [13] H. Cichoż-Lach, A. Michalak, Oxidative stress as a crucial factor in liver diseases, *World J. Gastroenterol.* 20 (25) (2014) 8082–8091. <https://doi:10.3748/wjg.v20.i25.8082>.
- [14] K. Jakubczyk, K. Dec, J. Kalduńska, D. Kawczuga, J. Kochman, K. Janda, Reactive oxygen species - sources, functions, oxidative damage, *Pol. Merkur. Lek.* 48 (284) (2020) 124–127.
- [15] A.K. Madiraju, Y. Qiu, R.J. Perry, Y. Rahimi, X.M. Zhang, D. Zhang, J.G. Camporez, G.W. Cline, G.M. Butrico, B.E. Kemp, G. Casals, G.R. Steinberg, D.F. Vatner, K.F. Petersen, G.I. Shulman, Metformin inhibits gluconeogenesis via a redox-dependent mechanism in vivo, *Nat. Med.* 24 (9) (2018) 1384–1394. <https://doi:10.1038/s41591-018-0125-4>.
- [16] L. Conde de la Rosa, T.E. Vrenken, M. Buist-Homan, K.N. Faber, H. Moshage, Metformin protects primary rat hepatocytes against oxidative stress-induced apoptosis, *Pharmacol. Res. Perspect.* 3 (2) (2015) e00125. <https://doi:10.1002/prp2.125>.
- [17] Y. Yan, C. Jun, Y. Lu, S. Jiangmei, Combination of metformin and luteolin synergistically protects carbon tetrachloride-induced hepatotoxicity: mechanism involves antioxidant, anti-inflammatory, antiapoptotic, and Nrf2/HO-1 signaling pathway, *BioFactors* 45 (4) (2019) 598–606. <https://doi:10.1002/biof.1521>.
- [18] G. Rahimi, S. Heydari, B. Rahimi, N. Abedpoor, I. Niktab, Z. Safaiejad, M. Peymani, F. Seyed Porootan, Z. Derakhshan, M.H.N. Esfahani, K. Ghaedi, A combination of herbal compound (SPTC) along with exercise or metformin more efficiently alleviated diabetic complications through down-regulation of stress oxidative pathway upon activating Nrf2-Keap1 axis in AGE rich diet-induced type 2 diabetic mice, *Nutr. Metab.* 18 (1) (2021) 14. <https://doi:10.1186/s12986-021-00543-6>.
- [19] M.F. Molina, M.N. Abdelnabi, T. Fabre, N.H. Shoukry, Type 3 cytokines in liver fibrosis and liver cancer, *Cytokine* 124 (2019) 154497. <https://doi:10.1016/j.cyt.2018.07.028>.
- [20] W.J. Zhang, S.J. Chen, S.C. Zhou, S.Z. Wu, H. Wang, Inflammasomes and fibrosis, *Front. Immunol.* 12 (2021) 643149. <https://doi:10.3389/fimmu.2021.643149>.
- [21] D. Cheng, J. Chai, H. Wang, L. Fu, S. Peng, X. Ni, Hepatic macrophages: key players in the development and progression of liver fibrosis, *Liver Int.* 41 (10) (2021) 2279–2294. <https://doi:10.1111/liv.14940>.
- [22] B. Hyun, S. Shin, A. Lee, S. Lee, Y. Song, N.J. Ha, K.H. Cho, K. Kim, Metformin down-regulates TNF- α secretion via suppression of scavenger receptors in macrophages, *Immune Netw.* 13 (4) (2013) 123–132. <https://doi:10.4110/in.2013.13.4.123>.
- [23] T. Tsuchida, S.L. Friedman, Mechanisms of hepatic stellate cell activation, *Nat. Rev. Gastroenterol. Hepatol.* 14 (7) (2017) 397–411. <https://doi.org/10.1038/nrgastro.2017.38>.
- [24] M.E. Guicciardi, G.J. Gores, Apoptosis as a mechanism for liver disease progression, *Semin. Liver Dis.* 30 (4) (2010) 402–410. <https://doi.org/10.1055/s-0030-1267540>.
- [25] C. Mitchell, M. Mahrouf-Yorgov, A. Mayeuf, M.A. Robin, A. Mansouri, B. Fromenty, H. Gilgenkrantz, Overexpression of Bcl-2 in hepatocytes protects against injury but does not attenuate fibrosis in a mouse model of chronic cholestatic liver disease, *Lab. Invest.* 91 (2) (2011) 273–282. <https://doi:10.1038/labinvest.2010.163>.
- [26] F. Xu, C. Liu, D. Zhou, L. Zhang, TGF- β /SMAD pathway and its regulation in hepatic fibrosis, *J. Histochem. Cytochem.* 64 (3) (2016) 157–167. <https://doi:10.1369/0022155415627681>.
- [27] M. Herranz-Iturbide, I. Peñuelas-Haro, R. Espinosa-Sotelo, E. Bertran, I. Fabregat, The TGF- β /NADPH oxidases Axis in the regulation of liver cell biology in health and disease, *Cells* 10 (9) (2021). <https://doi:10.3390/cells10092312>.
- [28] M. Roderfeld, S. Hemmann, E. Roeb, Mechanisms of fibrinolysis in chronic liver injury (with special emphasis on MMPs and TIMPs), *Z. Gastroenterol.* 45 (1) (2007) 25–33. <https://doi:10.1055/s-2006-927388>.
- [29] N. Argentou, G. Germanidis, P. Hytioglou, E. Apostolou, T. Vassiliadis, K. Patsiaoura, P. Sideras, A.E. Germenis, M. Speletas, TGF- β signaling is activated in patients with chronic HBV infection and repressed by SMAD7 overexpression after successful antiviral treatment, *Inflamm. Res.* 65 (5) (2016) 355–365. <https://doi:10.1007/s00011-016-0921-6>.
- [30] S.Y. Kwan, J. Jiao, A. Joon, P. Wei, L.E. Petty, J.E. Below, C.R. Daniel, X. Wu, J. Zhang, R.R. Jenq, P.A. Futreal, E.T. Hawk, J.B. McCormick, S.P. Fisher-Hoch, L. Beretta, Gut microbiome features associated with liver fibrosis in Hispanics, a population at high risk for fatty liver disease, *Hepatology* 75 (4) (2022) 955–967. <https://doi:10.1002/hep.32197>.
- [31] J. Pogorzelska, M. Łapińska, A. Kalinowska, T.W. Łapiński, R. Flisiak, Helicobacter pylori infection among patients with liver cirrhosis, *Eur. J. Gastroenterol. Hepatol.* 29 (10) (2017) 1161–1165. <https://doi:10.1097/meg.0000000000000928>.
- [32] A. Ponzetto, N. Figura, Helicobacter pylori infection among patients with liver cirrhosis, *Eur. J. Gastroenterol. Hepatol.* 30 (4) (2018) 490. <https://doi:10.1097/meg.0000000000001038>.
- [33] K. Atarashi, K. Honda, Microbiota in autoimmunity and tolerance, *Curr. Opin. Immunol.* 23 (6) (2011) 761–768. <https://doi:10.1016/j.coi.2011.11.002>.
- [34] J. Trottier, A. Bialek, P. Caron, R.J. Straka, P. Milkiewicz, O. Barbier, Profiling circulating and urinary bile acids in patients with biliary obstruction before and after biliary stenting, *PLoS One* 6 (7) (2011) e22094. <https://doi:10.1371/journal.pone.0022094>.
- [35] R. Mancinelli, L. Ceci, L. Kennedy, H. Francis, V. Meadows, L. Chen, G. Carpino, K. Kyritsi, N. Wu, T. Zhou, K. Sato, L. Pannarale, S. Glaser, S. Chakraborty, G. Alpini, E. Gaudio, P. Onori, A. Franchitto, The effects of taurocholic acid on biliary damage and liver fibrosis are mediated by calcitonin-gene-related peptide signaling, *Cells* 11 (9) (2022). <https://doi:10.3390/cells11091591>.
- [36] L. Caja, F. Diturì, S. Mancarella, D. Caballero-Díaz, A. Moustakas, G. Giannelli, I. Fabregat, TGF- β and the tissue microenvironment: relevance in fibrosis and cancer, *Int. J. Mol. Sci.* 19 (5) (2018). <https://doi:10.3390/ijms19051294>.
- [37] L. Timmers, J.P. Sluijter, J.K. van Keulen, I.E. Hoefler, M.G. Nederhoff, M.J. Goumans, P.A. Doevendans, C.J. van Echteld, J.A. Joles, P.H. Quax, J.J. Piek, G. Pasterkamp, D.P. de Kleijn, Toll-like receptor 4 mediates maladaptive left ventricular remodeling and impairs cardiac function after myocardial infarction, *Circ. Res.* 102 (2) (2008) 257–264. <https://doi:10.1161/circresaha.107.158220>.